Phys Chem Minerals (1991) 18:131–143

PHYSICS AND CHEMISTRY OF MINERALS

Mössbauer Study of the Thermal Decomposition of Lepidocrocite and Characterization of the Decomposition Products

P.M.A. de Bakker[1], E. De Grave[1,*], R.E. Vandenberghe[1], L.H. Bowen[2], R.J. Pollard[3], and R.M. Persoons[1,]**

[1] Laboratory of Magnetism, Gent State University, Proeftuinstraat 86, B-9000 Gent, Belgium
[2] Department of Chemistry, North Carolina State University, Box 8204, Raleigh, NC 27695, USA
[3] Department of Physics, Monash University, Clayton, Victoria 3168, Australia

Received December 14, 1990 / Accepted March 7, 1991

Abstract. The lepidocrocite (γ-FeOOH) to maghemite (γ-Fe_2O_3), and the maghemite to hematite (α-Fe_2O_3) transition temperatures have been monitored by TGA and DSC measurements for four initial γ-FeOOH samples with different particle sizes. The transition temperature of γ-FeOOH to γ-Fe_2O_3 and the size of the resulting particles were not affected by the particle size of the parent lepidocrocite. In contrast, the γ-Fe_2O_3 to α-Fe_2O_3 transition temperature seems to depend on the amount of excess water molecules present in the parent lepidocrocite. Thirteen products obtained by heating for one hour at selected temperatures, were considered. Powder X-ray diffraction was used to qualify their composition and to determine their mean crystallite diameters. Transmission electron micrographs revealed the particle morphology. The Mössbauer spectra at 80 K and room temperature of the mixed and pure decomposition products generally had to be analyzed with a distribution of hyperfine fields and, where appropriate, with an additional quadrupole-splitting distribution. The Mössbauer spectra at variable temperature between 4.2 and 400 K of two single-phase γ-Fe_2O_3 samples with extremely small particles show the effect of superparamagnetism over a very broad temperature range. Only at the lowest temperatures ($T \leq 55$ K), two distributed components were resolved from the magnetically split spectra. In the external-field spectra the $\Delta m_I = 0$ transitions have not vanished. This effect is an intrinsic property of the maghemite particles, indicating a strong spin canting with respect to the applied-field direction. The spectra are successfully reproduced using a bidimensional-distribution approach in which both the canting angle and the magnetic hyperfine field vary within certain intervals. The observed distributions are ascribed to the defect structure of the maghemites (unordered vacancy distribution on B-sites, large surface-to-bulk ratio, presence of OH^- groups). An important new finding is the correlation between the magnitude of the hyperfine field and the average canting angle for A-site ferric ions, whereas the B-site spins show a more uniform canting. The Mössbauer parameters of the two hematite samples with MCD_{104} values of respectively 61.0 and 26.5 nm display a temperature variation which is very similar to that of small-particle hematites obtained from thermal decomposition of goethite. However, for a given MCD the Morin transition temperature for the latter samples is about 30 K lower. This has tentatively been ascribed to the different mechanisms of formation, presumably resulting in slightly larger lattice parameters for the hematite particles formed from goethite, thus shifting the Morin transition to lower temperatures.

Introduction

As part of an on-going comprehensive research project concerning the determination of structural and magnetic properties of soil-related iron oxides and oxyhydroxides by means of ^{57}Fe Mössbauer spectroscopy, the thermal decomposition of single-phase, but poorly crystalline lepidocrocite, γ-FeOOH, has been investigated. In particular, this study was aimed to elucidate the correlation, if any does exists, between the characteristics of the resulting products on the one hand, and the crystallinity of the parent lepidocrocite on the other hand.

It is well known that γ-FeOOH, upon heating in air up to 300° C, decomposes into maghemite, γ-Fe_2O_3, which has a cation-deficient spinel structure. The ferric ions are distributed among the octahedral (B sites) and tetrahedral sites (A sites) of the spinel lattice. In most cases it is found that the vacancies occupy octahedral sites only (e.g. Haneda and Morrish 1977a; Greaves 1983), leading to the structural formula $(Fe)[Fe_{5/3}\square_{1/3}]O_4$, in which ( ) and [ ] represent A and B sites respectively, and □ stands for a vacancy. However, there is some indication (Annersten and Hafner 1973; Ramdani et al. 1987) that part of the vacancies

* Senior Research Associate, National Fund for Scientific Research (Belgium)
** Present Address: VITO, Boeretang 200, B-2400 Mol, Belgium

could be on A sites as well, at least for those maghemites prepared by oxidation of magnetite (Fe_3O_4).

At higher temperatures ($T \approx 350°$ C), γ-Fe_2O_3 transforms into hematite, α-Fe_2O_3. As discussed by Feitknecht and Mannweiler (1967), this phase transition, when it concerns small-particle maghemite (5.0 nm, which is the typical size for the samples obtained in the present study – see below), appears to be a chain mechanism in which some 50–100 neighbouring γ-Fe_2O_3 crystallites participate and are finally transformed into one large hematite particle. For large γ-Fe_2O_3 particles, the transition process evolves in a different manner. Recently, Sidhu (1988) studied the transformation of maghemite with particle diameter (according to electron microscopy) of approximately 100 nm. At 500° C, the γ- to α-Fe_2O_3 transition (GAT) is completed within 2 h, with no significant alteration of the particle size. For temperatures between 320 and 450° C, the transformation is very slow, and only 10% of the reaction was found to be completed in one week.

It is obvious that the proposed mechanism of hematite formation starting from small-particle maghemite, is different from the formation of hematite by dehydration of goethite α-FeOOH, and another main objective of the present work was to find out whether the Mössbauer parameters for α-Fe_2O_3 samples obtained by heating γ-FeOOH, show some distinctive features as compared to those previously measured for samples produced from α-FeOOH (De Grave et al. 1988).

The thermal decomposition of synthetic lepidocrocite has been studied before using, in addition to more conventional techniques such as electron and X-ray diffraction (Takada et al. 1964), ^{57}Fe Mössbauer spectroscopy (Subrt et al. 1981). A detailed quantitative interpretation of the Mössbauer spectra of the decomposition products of lepidocrocite has, however, not been attempted. In the present paper, we report the Mössbauer spectra at 80 K and RT and their numerical analysis, primarily in terms of hyperfine-field distributions, for a number of compounds obtained by heating four different γ-FeOOH samples at three to four different temperatures. Two single-phase maghemites and two hematites of different crystallinity were subsequently selected for a more profound study of their hyperfine parameters as a function of temperature between 4.2 and 400 K. In order to determine the precise cation distribution in the maghemite and to study to some extent the magnetic structure, data were additionally collected at 4.2 K in longitudinally applied magnetic fields of different strength.

Experimental

The preparation (from an aqueous Fe(II) sulfate solution at 45° C), the morphological characteristics and the Mössbauer spectra of the four parent lepidocrocite samples considered in this work, have been described in an earlier report (De Grave et al. 1986). Throughout the present paper, we will use the labels L65, L86, L121 and L147, the first one referring to sample P23 in (De Grave et al. 1986), to indicate the different lepidocrocites. The digits refer to the specific surface area SA in m^2/g as obtained from BET measurements. The *mean crystallite diameters* (MCD) along the b axis, estimated from the *X-ray diffraction* (XRD) line broadening, are respectively 44.0, 5.5, 6.0, and 3.0 nm and the excess of structural water molecules, expressed in number of H_2O molecules for each γ-FeOOH molecule, are respectively 0.07, 0.04, 0.10 and 0.02.

The thermal decomposition of the γ-FeOOH samples and the GAT were monitored by means of TGA and DSC measurements with a Dupont TGA-951 and DSC-910 set-up. The heating rate was 2° C/min. Samples were subsequently heated in air for one hour in an electrical furnace at selected temperatures in the range 250 to 600° C. The products obtained, labelled by the original lepidocrocite number followed by the heating temperature in °C, were further characterized by TEM and XRD. The diffraction patterns were recorded digitally with a resolution of 1/30° (2θ) per channel and afterwards computer fitted to a sum of Lorentzians or pseudo-Lorentzians, two for each reflection in order to account for the $K\alpha_1$ and $K\alpha_2$ radiation. In this way, the positions and broadenings of the relevant reflection lines could be determined with a relative accuracy of 0.01°.

Variable-temperature *Mössbauer spectra* (MS) of the decomposition products were collected with a time-mode spectrometer using a constant acceleration drive and a triangular reference signal. The absorbers contained an amount of material, mixed with very pure carbon, sugar or boron nitride, corresponding to 10 mg Fe/cm^2.

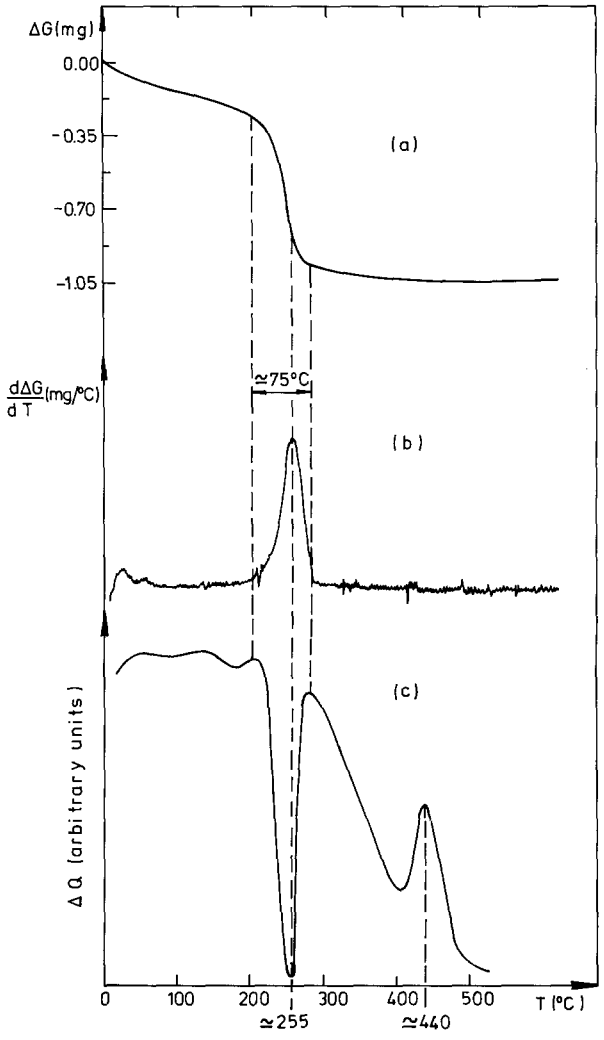

Fig. 1. (a) TGA, (b) DTGA and (c) DSC curves for lepidocrocite L86, showing the successive γ-FeOOH→γ-Fe_2O_3 and γ-Fe_2O_3→α-Fe_2O_3 transitions upon heating the sample at a rate of 2° C/min

Table 1. Mean crystallite diameter MCD_{hkl} in nm along the (hkl) lattice directions, estimated from the XRD line broadenings, for the α- and γ-Fe_2O_3 phases in the decomposition products of the lepidocrocite samples. The obtained products are indicated by the original lepidocrocite label followed by the heating temperature in °C

Sample	γ-Fe_2O_3			α-Fe_2O_3		
	(220)	(400)	(333)(511)	(104)	(110)	(300)
L65–337	7.0	11.0	5.5	20.5	u	35.0
L65–422	–	–	–	37.0	42.5	50.5
L65–546	–	–	–	61.0	72.5	71.0
L86–327	2.5	5.5	2.0	–	–	–
L86–488	–	–	–	22.5	34.5	31.5
L86–547	–	–	–	26.5	38.5	38.0
L121–303	2.0	4.5	3.0	–	–	–
L121–376	u	u	u	26.0	38.5	34.0
L121–560	–	–	–	39.5	44.5	67.5
L147–311	2.0	4.0	2.0	–	–	–
L147–380	2.0	5.0	2.5	4.0	u	8.0
L147–420	2.0	6.0	4.0	11.5	u	11.0
L147–606	–	–	–	29.5	34.0	35.5

u: reflections insufficiently resolved

The zero-field spectra were fitted either with a model-independent distribution of hyperfine fields based on the method of Wivel and Mørup (1981), or with one or two Lorentzian-shaped sextets. A model based on the simultaneous distribution of the intrinsic hyperfine field and the canting angle (de Bakker et al. 1990a), has been applied to interpret the external-field spectra of two selected maghemite samples and provided an adequate reproduction of the experimental line shape.

Results and Discussion

Characterization of the Samples

Figure 1 presents typical TGA and DSC curves for lepidocrocite L86. These are typical for all four γ-FeOOH samples. The loss of weight, starting at about 200° C (see Fig. 1a) marks the γ-FeOOH to γ-Fe_2O_3 transition around 250° C, which is an endothermic reaction as evidenced by the minimum in the DSC curve. This transition is not affected by the degree of crystallinity of the starting lepidocrocite. Small variations of 5° C between the four lepidocrocite samples for this transition temperature are within the experimental accuracy. The value found in this work is in reasonable agreement with most literature data (Bernal et al. 1957; Wolska and Baszynski 1986).

The maximum in the DSC curve around approximately 450° C (averaged over the four specimens) is the γ-Fe_2O_3 to α-Fe_2O_3 transition (GAT). The four investigated samples have a GAT at respectively 435, 450, 400 and 485° C, with an estimated error of 5° C. This variation in transition temperature is correlated with the amount of excess H_2O molecules found for the original lepidocrocites: the smaller this amount the higher the GAT-temperature seems to be. In contrast, Feitknecht and Mannweiler (1967) and Sidhu (1988) found the GAT-temperature to increase with increasing amount of residual Cl^--ions or with a small substitution of positive cations for Fe^{3+}-ions in the maghemite lattice. Furthermore the results of Farell (1972) indicate that the GAT-temperature decreases with increasing surface area. Such an unequivocal relation is not found for the present samples. Therefore, it is reasonable to state that the incorporation of OH^--ions in the maghemite lattice as a result of the excess water molecules in the parent lepidocrocite, has a marked infuence on the GAT, the defect structure favouring a lowering of the transition temperature by enhancing the transformation process.

Sidhu (1988) reported the GAT exotherm for maghemite particles with dimensions of the order of 100 nm to occur around 550° C. The higher heating rate applied by the author, i.e. 10° C/min, cannot account for the large difference with the present result (for a heating rate of 20° C, we found the temperature reading corresponding to the GAT exotherm to increase by not more than 50° C). As will be indicated below, the particle size of the maghemites dealt with in this paper, is smaller than 10 nm, and this poor crystallinity explains the observed, low average GAT temperature (Feitknecht and Mannweiler 1967; Farell 1972), whereas the amount of residual OH^--ions account for the scatter on the GAT-temperatures for the four investigated samples.

A total of 13 heated samples have been obtained for this investigation. They are listed Table 1, together with the qualitative compositions as derived from the XRD patterns, some of which are shown in Fig. 2. Since the variation in heating temperature for a given lepidocrocite sample is rather limited, it is not possible to define the phase boundaries for the γ and α modifications of ferric oxide within a reasonable uncertainty margin.

Figure 2 clearly shows that the diffraction peaks of α-Fe_2O_3 are much narrower than those for γ-Fe_2O_3, indicating a higher degree of crystallinity for the former. Table 1 lists the values of the MCD along certain crystallographic directions. They were estimated from the *full width at half maximum* (FWHM) of the corresponding diffraction lines using the Scherrer formula with K = 0.9 (Klug and Alexander 1974). The results for maghemite are found to be consistent with those of Berkowitz et al. (1968), who heated lepidocrocite up to 400° C and obtained γ-Fe_2O_3 particle sizes of less than 10 nm. Further, the considerable difference in crystallite size between the parent maghemite and hematite is consistent with the aforementioned chain mechanism for the GAT as suggested by Feitknecht and Mannweiler (1967). This mechanism also explains the observation that there is no correlation between the size of the maghemite particles and the size of the hematite particles produced from them. As for the γ-FeOOH to γ-Fe_2O_3 transition, the dimensions of the initial particles seem to remain unaltered for the L86, L121, and L147 starting materials. However, for L65, which has a much larger MCD_{020} value (44.0 nm) as compared to the three former lepidocrocites (3.0–6.0 nm), the initial particles seem to have been split into several smaller ones upon transforming to maghemite.

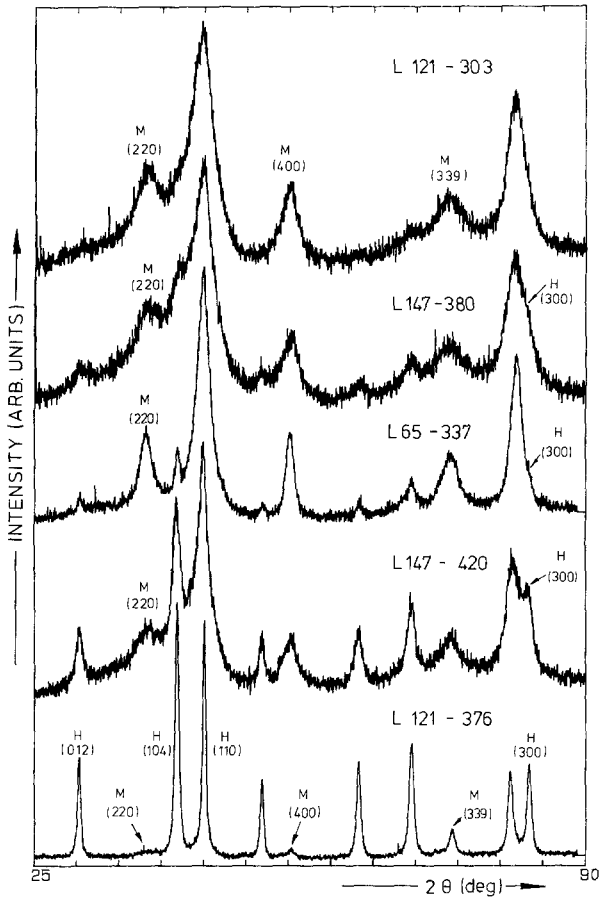

Fig. 2. X-ray diffraction patterns of some selected decomposition products. Relevant diffraction lines for maghemite (M) and hematite (H) are indicated.

Additional information concerning the samples' morphology was obtained from *transmission electron micrographs* (TEM). The average particle diameters for the four, single-phase hematite specimens L86–547, L147–606, L121–560 and L65–546 were estimated from the TEM's as 22, 37, 88 and 52 nm respectively and are in fair agreement with the data derived from the XRD line broadenings (see Table 1). The particles are almost spherically shaped and do not exhibit any macropores, in contrast to hematite prepared by thermal decomposition of goethite (Rendon et al. 1983; Verbeeck et al. 1986). The TEM for the maghemite sample shows a relatively large particle. Close inspection, however, shows a conglomerate of a large number of very small, needle-shaped crystallites. Takada et al. (1964) concluded from X-ray and electron diffraction experiments on maghemite crystallites (obtained from plate-like lepidocrocite by dehydroxylation) that the small γ-Fe_2O_3 crystallites with an average diameter of about 6.0 nm link together to form highly oriented aggregates whose shape resembles the morphology of the original lepidocrocite crystallites. This mechanism causes a strong magnetic interaction between the particles' ferrimagnetic moments (Berkowitz et al. 1968; Morrish and Clark 1974), which in turn leads to an enhanced hyperfine-field distribution interval, as evidenced by the large asymmetric broadening of the Mössbauer absorption lines at intermediate temperatures (Mørup 1983; Tamura and Hayashi 1988).

Mössbauer Spectroscopy

Some typical Mössbauer spectra obtained at RT and at 80 K are presented in Fig. 3 for the three distinct decomposition stages, i.e. single-phase γ-Fe_2O_3 (3a), a mixture of γ-Fe_2O_3 and α-Fe_2O_3 (3b and 3c), and single-phase α-Fe_2O_3 (3 d). The spectra have been described by a model-independent *magnetic hyperfine field distribution* (MHFD) and, where necessary, an additional *quadrupole splitting distribution* (QSD). The calculated line shapes (full lines) and the derived probability distribution profiles $p(H_{hf})$ of the MHFD are shown in Fig. 3 as well. The hyperfine parameters for the sextet components of the investigated decomposition products are listed in Table 2. For comparison, literature data for pure and well crystallized hermatite (Verbeeck et al. 1986) and for acicular maghemite particles with a length of 800 nm and a 6 to 1 shape ratio (Haneda and Morrish 1977b) have been included in the table. Note that for the latter one, the listed values of H_{hf} and δ are averages of the respective A- and B-site parameters. As indicated in Table 2, not all the involved spectra required a data analysis in terms of a MHFD: the hematite spectra, in particular those at 80 K, are observed to exhibit negligible asymmetric line broadening, and a more conventional fitting procedure was found to yield an acceptable goodness-of-fit. The distributed doublet component, observed at RT only for the samples L86–327, L121–303, L147–311, L147–380, and L147–420, has an isomer shift of 0.32 ± 0.01 mm/s against metallic iron and an average quadrupole splitting of 0.76 ± 0.02 mm/s, and is due to superparamagnetic maghemite particles.

Whereas in some instances the simultaneous presence of both α and γ modifications of Fe_2O_3 is obvious from the spectra at 80 K and/or at RT (e.g. sample L147–420 at RT, Fig. 3b and Table 2), this is not generally the case. A few examples will illustrate this. According to its XRD pattern (see Fig. 2), sample L65–337 contains a minor amount of hematite, probably of the order of 10%. However, neither the shape of the Mössbauer spectra and the derived MHFD histograms at 80 K or at RT (Fig. 3c), nor the iterated hyperfine parameters (Table 2), provide any indication of the presence of hematite. A similar observation holds for α- and γ-Fe_2O_3 mixtures at the other end of the compositional range, e.g. L121–376 (see Fig. 2, bottom pattern) which contains a small amount of the γ modification. The Mössbauer data, however, suggest a pure hematite compound with a rather high crystallinity since its spectrum at 80 K, with $2\varepsilon_Q = 0.38$ mm/s, is not composed of a *weakly-ferromagnetic* (WF) and an *antiferromagnetic* (AF) contribution, as is the case for less crystalline hematites (De Grave et al. 1983).

In conclusion, mixtures of hematite and maghemite, such as those resulting from the decomposition of lepidocrocite, are not readily characterized by means of Mössbauer spectroscopy at temperatures in the range

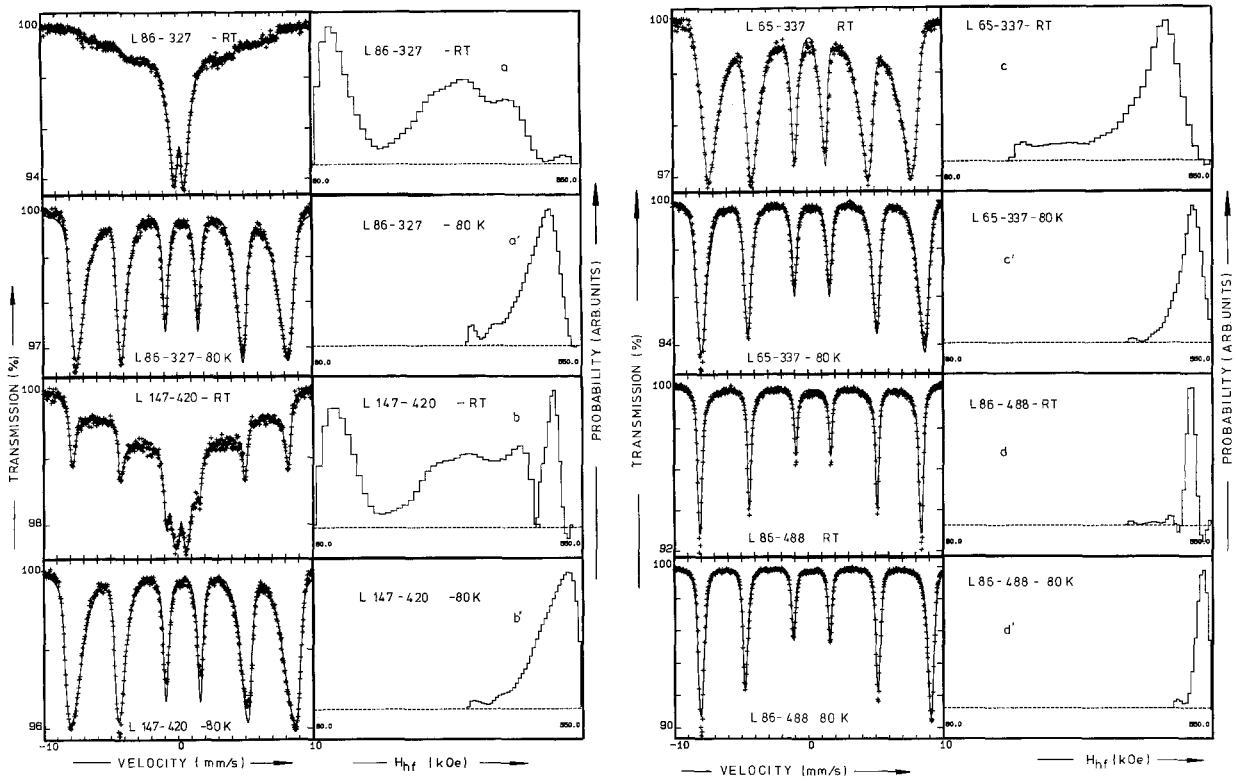

Fig. 3. Mössbauer spectra at RT and 80 K of a pure maghemite (a), a mixture of maghemite and hematite (b)(c) and a pure hematite (d). The corresponding magnetic hyperfine-field distributions are given as well

Table 2. Average hyperfine field $\bar{H}_{hf}$, field of maximum probability H_{hf}^{m}, quadrupole shift $2\varepsilon_Q$ and isomer shift δ versus metallic iron of the hyperfine-field distributions fitted to the spectra at 80 K and at RT of the decomposition products of lepidocrocite, and identification (ID) (h = hematite, m = maghemite) suggested by these data. For comparison, literature data for single-phase, well crystalline hematite and maghemite are indicated as well (single-sextet fits)

Sample	80 K				RT				ID
	$\bar{H}_{hf}$ (kOe)	H_{hf}^{m} (kOe)	$2\varepsilon_Q$ (mm/s)	δ (mm/s)	$\bar{H}_{hf}$ (kOe)	H_{hf}^{m} (kOe)	$2\varepsilon_Q$ (mm/s)	δ (mm/s)	
α-Fe_2O_3	542		0.35	0.47	518		−0.21	0.37	
γ-Fe_2O_3	517		≈0.0	0.40	500		≈0.0	0.32	
L65–337	507	517	0.03	0.45	419	468	0.01	0.32	m
L65–422*	539		0.30	0.48	516	518	−0.21	0.36	h
L65–546*	540		0.36	0.47	516	518	−0.21	0.37	h
L86–327	470	493	0.01	0.44	269	346	0.00	0.33	m
L86–488	530	533	0.31	0.49	505	513	−0.21	0.36	h
L86–547*	538		0.33	0.47	505	510	0.21	0.36	h
L121–303	479	498	0.01	0.44	274	368	−0.00	0.30	m
L121–376	529	533	0.38	0.49	510	514	−0.21	0.37	h
L121–560*	540		0.34	0.48	515	516	−0.21	0.36	h
L147–311	446	492	−0.01	0.44	226	318	0.01	0.36	m
L147–380	466	487	−0.01	0.44	245	346	−0.01	0.31	m
L147–420**	494	526	−0.03	0.47	276	351	−0.03	0.31	m+h
					494	499	−0.20	0.36	
L147–606	539		0.34	0.48	507	511	−0.21	0.36	h

* 80 K spectra fitted with a single sextet
** RT spectrum fitted with two magnetic hyperfine field distributions

80 to 300 K, in particular when one of the constituents is present in minor concentrations.

Mössbauer spectroscopy on two selected maghemite samples. The two single-phase maghemite samples L121–303 and L147–311 were selected for a study of the temperature dependence of the Mössbauer effect. Preliminary, but substantially incomplete results have been included in an earlier report of this laboratory (de Bakker et al. 1990b). A collection of spectra with the corresponding MHFD profiles is presented in Fig. 4 and refers to sample L121–303. The results are listed in Table 3. A superimposed QSD (tentatively chosen to be in the range 0.0 to 1.5 mm/s) was found to be required for L121–303 at $T \geq 160$ K and for L147–311 at $T \geq 130$ K. The average quadrupole splitting was calculated to be within

Table 3. Temperature dependence of the hyperfine parameters of maghemite sample L121–303. Average hyperfine field $\bar{H}_{hf}$, field of maximum probability H_{hf}^{m}, distribution half-width σ_H, quadrupole shift $2\varepsilon_Q$, isomer shift δ versus metallic iron and the relative area (RA) of the magnetic hyperfine-field distributions

L121–303

T (K)	Site	$\bar{H}_{hf}$ (kOe)	H_{hf}^{m} (kOe)	σ_H (kOe)	$2\varepsilon_Q$ (mm/s)	δ (mm/s)	RA (%)
4.2	A	486	494	16	−0.04	0.37	28
	B	517	520	11	−0.01	0.46	72
12	A	484	500	20	−0.04	0.36	27
	B	515	520	13	−0.00	0.46	73
30	A	486	501	21	−0.03	0.36	37
	B	514	518	13	−0.01	0.46	63
55	A	475	480	20	−0.08	0.38	39
	B	510	510	12	−0.01	0.44	61
80	A+B	478	498	36	0.01	0.44	100
100	A+B	470	494	40	−0.00	0.43	100
130	A+B	447	489	53	−0.00	0.41	100
160	A+B	397	469	99	−0.00	0.39	97
190	A+B	356	451	113	−0.00	0.38	95
220	A+B	327	429	120	−0.02	0.35	91
250	A+B	296	297	123	−0.01	0.33	86
280	A+B	283	359	123	−0.01	0.32	80
310	A+B	273	345	122	−0.01	0.31	75
340	A+B	266	342	121	−0.01	0.28	71
370	A+B	260	345	120	−0.00	0.27	67
400	A+B	256	335	119	−0.00	0.26	65

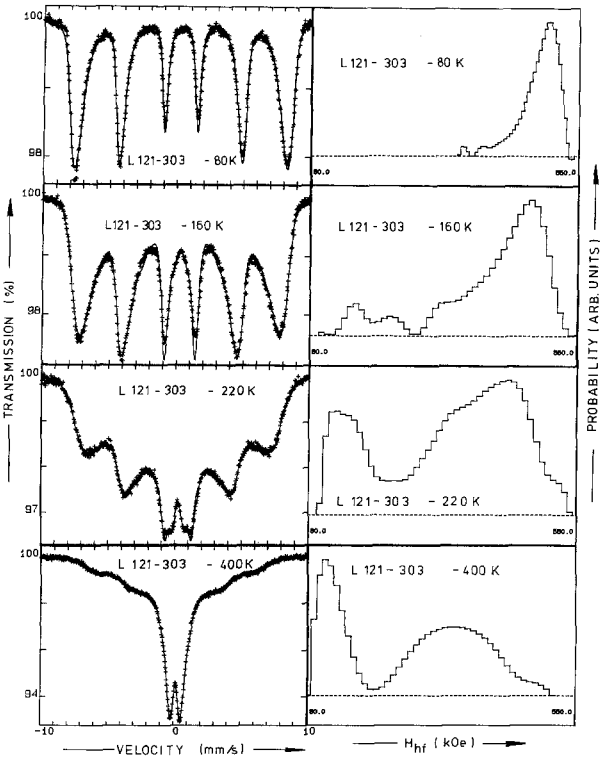

Fig. 4. Mössbauer spectra of maghemite L121–303 at some selected temperatures. The full line is the calculated spectrum. The corresponding magnetic hyperfine-field distributions are given as well

0.77 ± 0.01 mm/s and seems not to be affected by temperature. The isomer shift of the doublet component was found to coincide with the value iterated for the MHFD to within 0.01 mm/s, which is within the experimental error limits. The relative contribution of the QSD component to the total spectrum gradually increases with increasing temperature from 3% at 160 K to 35% at 400 K for L121–303 and from approximately 5% at 130 K to 95% at 400 K for L147–311. These figures, however, are not very accurate due to the strong overlap with low-field magnetic components.

The central doublet component observed in the reported spectra of both maghemites, is due to superparamagnetic γ-Fe_2O_3 particles. An impurity phase was not detected with Mössbauer spectroscopy nor with X-ray diffraction, and the presence of an amorphous iron oxide is ruled out by the relatively high heating temperature. From extrapolation of the linear part of the curve representing the relative doublet area as a function of the measuring temperature, the blocking temperature T_B could be derived as the intersection with the 0% doublet fraction line. T_B for the present maghemite systems is estimated to be 160 K and 130 K for L121–303 and L147–311 respectively, which is in reasonable agreement with the results obtained by Picone et al. (1982) and by Coey and Khalafalla (1972) for maghemites with average particle sizes of less than 10 nm.

From the shape of the Mössbauer spectra (Figs. 4, 5), it is clear that even at low temperatures H_{hf} exhibits a broad range of values, reflecting a wide distribution in particle size with a very low average volume. For such a small-particle system, intra-particle collective magnetic excitations (Mørup and Topsøe 1976) and inter-particle magnetic interactions (Mørup 1983) caused by the clustering of the γ-Fe_2O_3 crystallites, indeed reduce the H_{hf} of an individual particle by an amount depending on its volume and on the temperature. For a real sample at a given temperature below the blocking temperature, fields anywhere between zero and the maximum value at that temperature can theoretically be expected. These field-reducing effects, however, are not important at 4.2 K since the derived theoretical expressions predict a zero field reduction at zero Kelvin. Hence, the observed remaining, but relatively narrow MHFD at 4.2 K must be due to other phenomena. In this respect, a characteristic feature of the involved γ-Fe_2O_3 compounds is the large surface area, meaning that a considerable fraction of the iron species somehow must be affected by the surface. Due to e.g. missing exchange paths (Batis-Landoulsi and Vergnon 1983), the hyperfine field near the surface is generally smaller than the bulk value. Such reduction has been demonstrated frequently for various Fe oxides using a variety of surface-sensitive techniques based on the Mössbauer effect (Haneda and Morrish 1977b; Ochi et al. 1981; Brett and Graham 1986).

Other effects which likely contribute to the distributive nature of the Mössbauer spectra at very low temperatures include the change in strength and asymmetry of the quadrupole interaction in going from the inner part of the particles towards their surface (De Grave et al. 1986), the presence of OH^- groups (Morrish and

Clark 1974) and the unordered distribution of vacancies on the B sublattice (Haneda and Morrish 1977a). This latter feature causes a distribution on the A-site supertransferred hyperfine field which for spinel ferrites ranges between 0 and ≈ 40 kOe depending on the number of nearest-neighbour Fe_B^{3+} ions (Vandenberghe and De Grave 1989).

As mentioned in the Introduction, the ferric ions in maghemite are situated on two, crystallographically different lattice sites, and therefore two distinct Zeeman patterns are to be expected. Due to the small differences in hyperfine parameters and to the distribution of these parameters, the two components could only be resolved from the spectra taken at the lowest temperatures ($T \leq 55$ K). The obtained relevant A- and B-site hyperfine parameters for sample L121–303 are listed in Table 3 and are in line with what is generally observed for spinel ferrites (Vandenberghe and De Grave 1989), including well crystalline γ-Fe_2O_3 (Pollard and Morrish 1987). The A-site hyperfine field distribution seems to be consistently broader than the B-site one, which could be explained by the above mentioned supertransfer mechanism. However, it cannot be excluded that this effect originates from the overestimation of the A-site low-field contributions due to the residual overlap with the B-site pattern.

Although the low-temperature spectra are adequately described by two independent MHFDs, each with reasonable hyperfine parameter values, the calculated relative areas S_A and S_B (see Table 3) are not always acceptable on the basis of structural considerations: because maghemite is a spinel with 1/3 of its normally occupied octahedral sites replaced by vacancies, the expected values for S_A and S_B are 37.5% and 62.5% respectively.

At high temperatures ($T \geq 80$ K), only one single MHFD can be adjusted and hence the evaluated parameters are averages for A and B sites. The experimental line shape of the high-temperature spectra is quite reasonably reproduced, but, the high probabilities obtained for hyperfine fields $H_{hf} \leq 200$ kOe are believed to be unrealistic for reasons mentioned earlier. Further, the outer absorption lines at intermediate temperatures are clearly asymmetric, which is not accounted for in the calculated spectrum. Other shortcomings of the fitting model may be noticed and it is believed that most of these are a consequence of approximating two MHFD's, with unequal isomer shifts, by a single one. Nevertheless, it is obvious that for both maghemites the hyperfine field distributions are extremely broad and the coexistence of sextet and doublet components persists over a very extensive temperature region. These features are to some extent in disagreement with the theoretical considerations of Mørup (1983) which predict the suppression of superparamagnetic relaxation for strongly interacting magnetic particles, and also with the Mössbauer experiments of Koch et al. (1986) on small-particle goethites and of Jing et al. (1990) on nanocrystalline hematite which do seem to satisfy, at least qualitatively, Mørup's theory. This different behaviour of the various iron oxides and oxyhydroxides remains unexplained at the moment.

A selection of external-field spectra (4.2 K) is shown in Fig. 5 for L147–311. Since maghemite is ferrimagnetic, the magnetic moment at the octahedral sites being the largest, the external field H_{ext} adds to the A-site hyperfine fields and subtracts from the B-site fields, so that the difference between the average effective fields

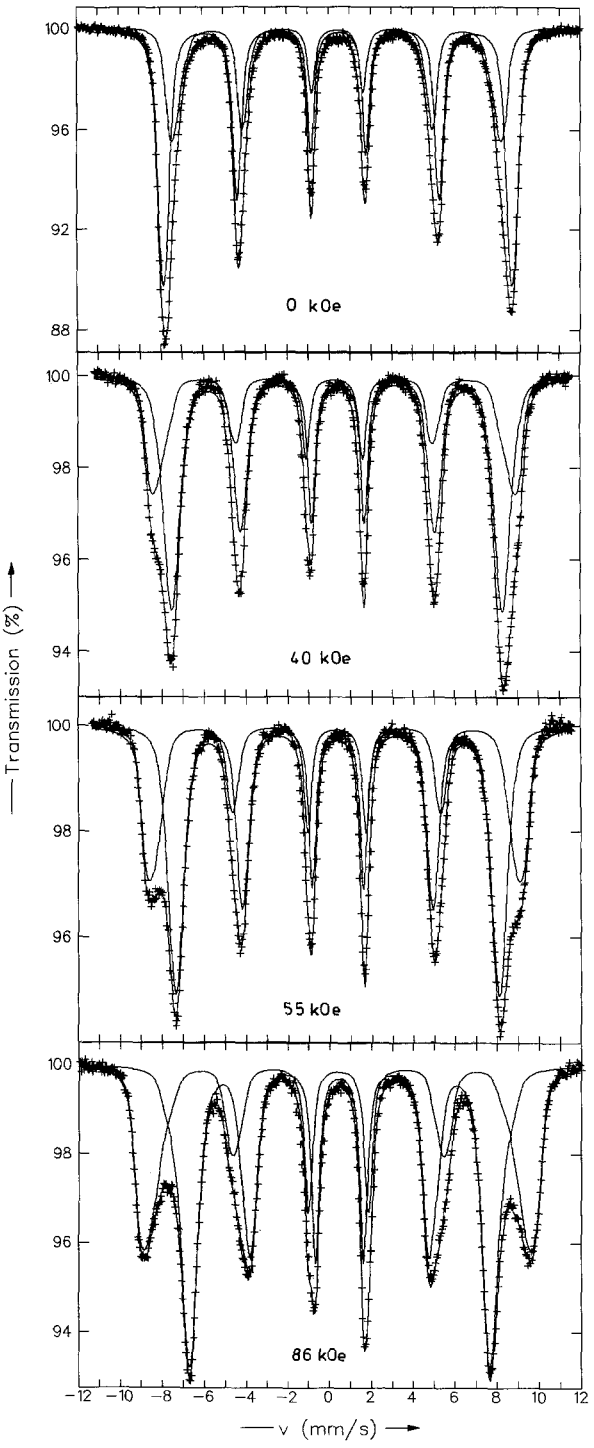

Fig. 5. Mössbauer spectra of maghemite L147–311 collected at 4.2 K without external field and in fields of different strengths as indicated. The zero-field spectrum is analysed with the conventional hyperfine-field distribution, whilst the external-field spectra are analysed according to the bidimensional distribution method. The full lines represent the calculated subspectra and their sum

Table 4. Hyperfine parameters obtained from the bidimensional distribution fit of the spectra of the two maghemite samples, collected in external fields of different strength. Average hyperfine field $\bar{H}_{hf}$, field of maximum probability H^m_{hf}, one-dimensional distribution half-widths σ_H and σ_θ, average and maximum canting angle $\bar{\theta}$ and θ^m, quadrupole shift $2\varepsilon_Q$, isomer shift δ versus metallic iron and relative area (RA) of both subspectra. H^b_{hf} and H^e_{hf} are the upper and lower hyperfine-field limits. All spectra have been collected at 4.2 K, except L121–303 in a field of 60 kOe, for which the absorber temperature was 10 K

H_{ext} (kOe)		H^b_{hf} (kOe)	H^e_{hf} (kOe)	$\bar{H}_{hf}$ (kOe)	H^m_{hf} (kOe)	σ_H	$\bar{\theta}$ (°)	θ^m (°)	σ_θ (°)	$2\varepsilon_Q$ (mm/s)	δ (mm/s)	RA (%)
L121–303												
0	A	430	515	486	494	16	–	–	–	−0.04	0.37	28
	B	480	540	517	520	11	–	–	–	−0.01	0.46	72
60	A	460	535	504	509	14	41	35	20	−0.07	0.38	39
	B	465	545	519	525	15	138	142	17	0.01	0.48	61
84	A	430	525	501	510	16	41	40	22	−0.05	0.38	41
	B	460	535	515	522	13	142	146	18	0.01	0.48	59
L147–311												
0	A	430	510	480	489	16	–	–	–	−0.02	0.41	36
	B	490	540	515	516	10	–	–	–	−0.01	0.47	64
40	A	460	540	492	503	18	46	58	22	−0.05	0.36	43
	B	465	550	518	523	18	134	137	17	−0.04	0.51	57
55	A	435	525	498	510	18	46	51	19	−0.05	0.39	40
	B	465	540	516	524	15	134	136	16	−0.00	0.47	60
86	A	425	525	493	504	19	45	45	20	−0.05	0.40	41
	B	450	530	510	516	14	136	143	19	−0.00	0.48	59

H_{eff} felt by the tetrahedral and octahedral ferric ions becomes considerably larger. Further, if the magnetic structure were collinear, as in well crystallized maghemite, the $\Delta m_I = 0$ absorption lines (i.e. lines 2 and 5) should be absent. This is clearly not the case for these poorly crystalline maghemites.

The presence of the $\Delta m_I = 0$ transitions in the external-field spectra of small-particle maghemite is well documented. Coey (1971, 1987) and Coey and Khalafalla (1972), who studied samples with average particle diameter of 5.0–7.5 nm, proposed that the effect is due to a random canting of the surface spins. Morrish et al. (1976) and Pollard and Morrish (1987) measured the spectra in fields of 5T for samples with a grain size of at least one order of magnitude larger and observed a much smaller effect. From the relative areas of the middle lines, they evaluated the average spin canting angle, which turned out to be the same for A and B sites and ranged between 13 and 30 degrees depending on the particle size. More recently, Pollard (1990) repeated his earlier measurements, however in stronger external fields (9T) and with extremely high counting statistics. He argued that the middle lines earlier assigned to A-site canting actually are due to an impurity hematite phase, which is antiferromagnetic at low temperatures and hence whose line positions and intensities are not drastically affected by magnetic fields of moderate strength. The presence of hematite could indeed be detected in the XRD patterns. The author concluded that the A-site spins are aligned completely antiparallel to the field direction, whereas the B-site spins are canted by an amount decreasing slightly with increasing field strength.

As for the present γ-Fe_2O_3 samples, no indication whatsoever could be found for the presence of any significant amount of α-Fe_2O_3. As reported in detail in an earlier paper (de Bakker et al. 1990b), the analysis of the applied-field spectra on the basis of two hyperfine-field distributions or on the basis of two broadened components, each with a distribution of the canting-angle, did not yield reasonable fitting results. On the contrary, the use of a simultaneous distribution of the intrinsic hyperfine field H_{hf} and the angle θ between H_{hf} and H_{ext} (de Bakker et al. 1990a) for both A and B sites, showed a major improvement of the goodness-of-fit. As seen from Fig. 5, the experimental line shapes are remarkably well reproduced by the calculations (full lines). The adjusted parameter values were observed to depend slightly on the specified lower and upper limits of the field range, (H^b_{hf}, H^e_{hf}), especially for the lower H_{ext} values. Many different field intervals, each containing 15 increments, were tried out. In all cases, the angle distribution varied from 0° to 90° for the A-site subspectra and from 180° to 90° for the B-site ones, each in steps of six degrees. The width of the elementary sextet contributions was fixed at 0.38 mm/s. The final results as summarized in Table 4, were selected on the basis of three criteria: the goodness-of-fit, the smoothness of the obtained bidimensional distributions and the evaluated value of the area ratio of the two components, which we wanted to be as close as possible to the ideal 37:63 ratio, the Mössbauer fractions for both sites approaching unity at 4.2 K (Vandenberghe and De Grave 1989). The consistent overestimation of this ratio (see Table 4) might be fortuitous and within the error limits of the data analyses. It could, however, indicate a higher-than-ideal vacancy concentration on B sites as was recently pointed out by Goss (1988) and this would be consistent with the presence of residual hydroxyl groups in the spinel lattice as observed from IR spectroscopy (Wolska and Baszynski 1986). In any case, according to these results it seems very unlikely that a significant amount of vacancies is present on the tetrahedral sublattice.

The fluctuations of the hyperfine-field values for a

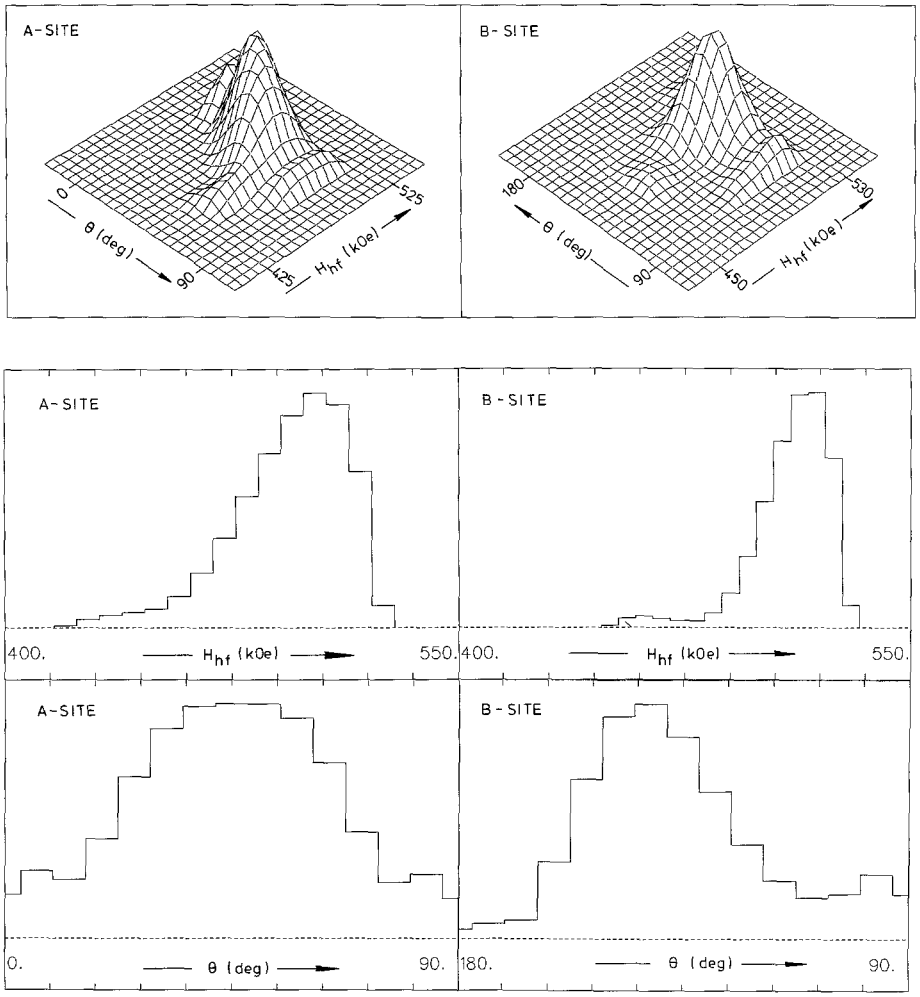

Fig. 6. The bidimensional distribution profiles for both sites obtained from the 4.2 K spectrum of maghemite L147–311 in an external field of 86 kOe (top). The integrated one-dimensional hyperfine-field and canting-angle distribution profiles for both A- and B-sites (bottom) are given as well

given sample in different applied fields (see Table 4) reflect the inaccuracy of the calculations. Taking into account this error, both the average and maximum-probability fields of L147–311, which has the smallest particle size, are smaller than those for L121–303. The observed difference (5 ± 3 kOe) is in line with the difference between the present results and the average hyperfine-field values obtained for particles of $350 \times 35 \times 35$ nm^3, i.e. 514 kOe and 533 kOe for A and B sites respectively (Pollard and Morrish 1987). In general, the distribution of fields is broader for A sites than for B sites which is consistent with the results obtained for the spectra collected without applied field. The same tendency is observed for the distribution of canting angles. The average canting is somewhat more pronounced for the smaller L147–311 maghemite and is apparently not affected by the strength of the applied field.

The bidimensional (H_{hf}, θ) distribution and the corresponding integrated one-dimensional distribution profiles for both A- and B-sites of sample L147–311 in an external field of 86 kOe are presented in Fig. 6. In general, the H_{hf} distributions derived from the in-field spectra are in fair agreement with those obtained from the zero-field spectra. For each considered field value between the limits of the field range, the corresponding average canting angles were calculated as well. The results are shown in Fig. 7 and refer to the highest applied fields. Similar dependences were evaluated for the 60 (55) kOe runs, but due to the poorer separation of the A- and B-site patterns, there is more scatter in the data and it is uncertain whether the apparent differences with the curves in Fig. 7 are realistic.

An important conclusion from Fig. 7 is that the average canting angle for the B-site spins is more or less uniform, whereas for the A sites a correlation with the hyperfine field is obvious: smaller field values are associated with a more pronounced average canting. This correlation could be related to the presence of structural defects such as the nearest-neighbour vacancy concentration on B-sites (which has a more pronounced effect on the A-site hyperfine fields than on the B-site ones) and of OH^- groups in the anion lattice, missing exchange paths in the surface layers. However, the question then arises why similar effects do not occur for the B-site spins. At the moment, a straightforward answer to this question cannot be given. Nevertheless, the observed features suggest a very complicated and highly disordered spin structure for these nanocrystalline maghemites.

Finally, it should be mentioned that the average canting angles from the adjusted bidimensional distribution are in remarkable agreement with the results of Morrish

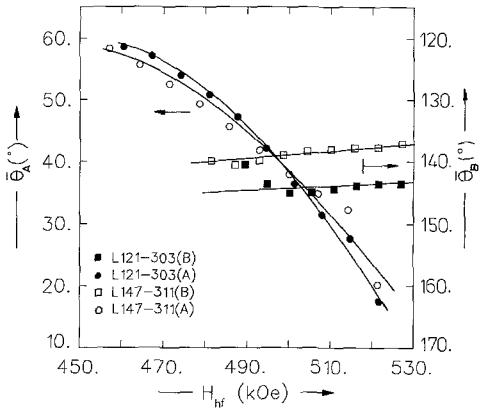

Fig. 7. Calculated average canting angle versus hyperfine field for A- and B-sites obtained from the spectra of both maghemite samples collected in the highest applied fields

Table 5. Hyperfine parameter data obtained from the temperature dependence of the various Mössbauer parameters for the two hematite samples. The subscripts AF and WF refer to the antiferromagnetic and weakly ferromagnetic contributions to the total spectrum. $H_{hf,AF}(0)$ is the saturation value for the magnetic hyperfine field of the low-temperature antiferromagnetic phase. J_e is the antiferromagnetic inter-sublattice exchange interaction. $2\varepsilon_{Q,AF}(0)$ and $2_{Q,WF}(0)$ are the saturation values of the quadrupole shift, δ_I the intrinsic isomer shift, relative to metallic iron, θ_M is the characteristic Mössbauer temperature appearing in the Debye approximation for the temperature dependence of the isomer shift, T_M is the Morin transition temperature and $RA_{WF}(0)$ the relative spectral area of the weakly-ferromagnetic component at zero Kelvin

	L65–546	L86–547
$H_{hf,AF}(0)$ (kOe)	541.0 (9)	539.0 (6)
J_e (K)	28 (2)	32 (3)
$2\varepsilon_{Q,AF}(0)$ (mm/s)	0.36 (1)	0.35 (1)
$2\varepsilon_{Q,WF}(0)$ (mm/s)	−0.21 (2)	−0.21 (2)
δ_I (mm/s)	0.610 (5)	0.613 (5)
θ_M (K)	500 (10)	529 (10)
T_M (K)	245 (5)	215 (5)
$RA_{WF}(0)$	0.00	0.13

The figures between brackets are three times the standard deviations

et al. (1976) for surface-enriched γ-Fe_2O_3 (particle dimensions exceeding 100 nm). For the surface spins, these authors indicate canting angles with respect to the external field of 58° and 133° for A and B sites respectively. This conclusion was later confirmed by Okada et al. (1983) using emission Mössbauer spectroscopy of ^{57}Co adsorbed on γ-Fe_2O_3 particles with similar particle sizes. These authors further suggest that the spins in the core part of the grains are completely aligned. As for the present maghemites, the obtained results imply that canting occurs throughout the whole particle and this feature can be explained by the much smaller size of the involved crystallites.

Mössbauer spectroscopy on two selected hematite samples. The two hematite samples selected for the subsequent part of this study were L65–546 and L86–547. Spectra were taken at ascending temperatures between 80 and 400 K in steps of 10–20°. They were analyzed as described in De Grave and Vandenberghe (1990), except for temperatures exceeding RT for which a narrow hyperfine-field distribution was considered in order to account for the distribution in particle sizes. The relevant quantities obtained from the data analyses are listed in Table 5 and are in line with previously reported results for natural and synthetic hematites with and without substitution. The saturation values $H_{hf,AF}$ (0) of the hyperfine field for the antiferromagnetic state were obtained by least-squares fitting or the expression:

$$\frac{H_{hf}(T)}{H_{hf}(0)} = 1 - 1.59\ 10^{-3} \cdot \frac{k^2\,T^2}{(2J_e)^2} \qquad \left(\frac{T}{T_N} < 0.5\right) \qquad (1)$$

which originates from Kubo's spin-wave theory for magnetic ions coupled antiferromagnetically to six nearest neighbours (Kubo 1952). The parameter J_e in (1) is the exchange integral quantifying the strength of the interaction between two magnetic ions. The values as indicated in Table 5 may be somewhat overestimated due to an additional temperature dependence of $H_{hf,AF}$ arising from the thermally activated collective excitations of the particles' magnetic moments (Mørup and Topsøe 1976).

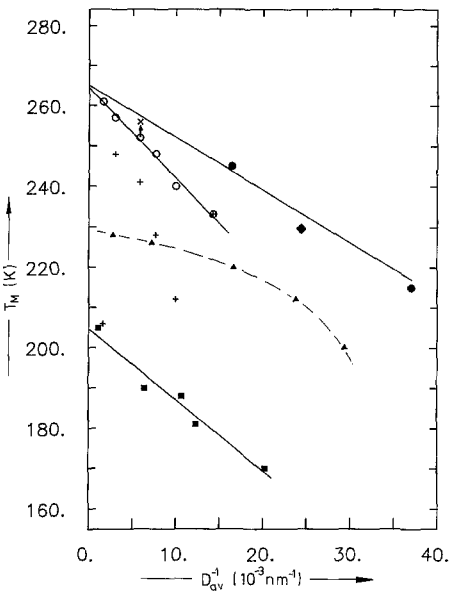

Fig. 8. A collection of previously published Morin transition temperatures T_M for different hematite samples as a function of the inverse of the average particle diameter D_{av} obtained from XRD measurements or TEM photographs (■) Al-substituted hematite obtained by decomposition of aluminous goethites (De Grave et al. 1988), (▲) hematites obtained by heating an unsubstituted goethite at different temperatures (Verbeeck et al. 1986), (◆) natural hematite (sample H3) from the region of Elba (De Grave and Vandenberghe 1990), (●) present results for hematites obtained by heating lepidocrocites above 500° C and hematites prepared from metal hydrous oxid sols (+) and afterwards heated at 300° C (○) (Amin and Arajs 1987). These latter T_M values have to be corrected in order to be comparable with the definition of T_M as given in this work. The corrected value yields a data point (×), which is more in line with the present results

Since the presently obtained data are very similar to those reported earlier for other hematite samples (De Grave et al. 1988), there is no need to discuss them in detail. The only parameter which deserves some attention here, is the Morin-transition temperature, T_M, as usual defined as the temperature at which the AF contribution to the total spectrum is reduced to one half of its saturation value. Figure 8 contains a selection of previously published T_M values for hematites. The data are plotted against the inverse of the average particle dimensions obtained either from XRD line broadening (MCD) or from TEM. The results of Amin and Arajs (1987), however, cannot be compared directly with those of the other α-Fe_2O_3 samples since they refer to the lower limit of the temperature region in which the spin reorientation evolves. For one case, for which the magnetization versus temperature curves are shown in detail in their paper, one can derive the value of T_M as defined in the way indicated above. This yields a data point ($\times$ in Fig. 8) which is more in line with the results for the natural compound (filled diamond) and for the samples obtained from maghemites (filled circles).

Figure 8 clearly demonstrates that the Morin transition in hematite to some extent depends on the history of the sample. The samples prepared from goethite exhibit the lowest T_M values. This is not due to the macropores since their presence is reflected in the magnitude of the MCD. Moreover, the pores have vanished after annealing at the highest temperature (900° C – left-most triangle in Fig. 8), but T_M still does not exceed 230 K, which is significantly lower than for the smaller L65–546 particles. For a given MCD value, T_M for the hematites obtained from α-FeOOH is on the average 30° lower than for the ones obtained from γ-FeOOH. It is not believed that this could be an effect of a lower concentration of hydroxyl groups in the latter samples since their temperature of formation was much lower.

It is very likely that the shift between the Morin-transition temperatures for the two hematite groups is directly related to the different mechanism of formation of the particles. These mechanisms have been described by Feitknecht and Mannweiler (1967) for γ-$Fe_2O_3 \rightarrow$ α-Fe_2O_3 and by Feitknecht and Michaelis (1962) for α-FeOOH$\rightarrow\alpha$-Fe_2O_3. More recently, Watari et al. (1979, 1982) have demonstrated that the dehydroxylation reaction from goethite produces aggregates of well-oriented twin-related hematite crystals, separated by regularly spaced walls of voids. Such a mosaic structure is not expected to occur during the growth from maghemite crystals.

In this respect, the observed features as displayed in Fig. 8 can be explained as follows. The different structure of the α-Fe_2O_3 crystals is suggested to imply slighty different lattice parameters. It is well known that the Morin transition is extremely sensitive to changes in the lattice parameters. This has been established by the high-pressure Mössbauer work of Vaughan and Drickamer (1967) and of Bruzzone and Ingalls (1983), who both found a significant increase in T_M with increasing pressure, i.e. with decreasing inter-atomic distances (Lewis and Drickamer 1966). According to the results of Ninginger and Schroeer (1978), a minute lattice dilatation of 0.03% causes T_M to drop by approximately 20 K. Muench et al. (1985) measured the temperature variation of the magnetization for spherical hematite particles with varying diameter d and derived an emphirical correlation between T_M on the one hand, and the relative lattice dilatation ε and particle size d on the other hand. From this, it can be deduced that the downward shift ΔT_M can be approximated by:

$$\Delta T_M = 600\varepsilon + 1.3\ 10^3/d$$

with d in nm and ε in %. The upper solid line in Fig. 8 has a slope of $1.35\ 10^3$ Knm. In order to explain the average drop of 30 K of the other group of hematites (broken curve), a change in the dilatation of 0.05% with respect to the present hematites has to be concluded. Unfortunately, the available XRD equipment was not sufficiently precise to measure line shifts corresponding to such a small effect.

Conclusions

A detailed quantitative Mössbauer investigation of the decomposition products of four synthetic, poorly crystalline lepidocrocite samples has been attempted. Determination of the lepidocrocite to maghemite, and of the maghemite to hematite transition temperatures has been achieved by TGA and DSC measurements. The transition from lepidocrocite to maghemite was not affected by the particle size of the parent lepidocrocite. In contrast, the maghemite to hematite transition temperature showed a remarkable dependence upon the amount of excess water molecules present in the parent lepidocrocite. It is believed that the substitution of OH^- groups in the maghemite anionic lattice enhance this transition. XRD measurements were used to obtain information on the composition of the decomposition products and their mean crystallite diameters. TEM photographs revealed the morphology of the samples. The Mössbauer spectra of the mixed and pure decomposition products generally had to be analyzed with a distribution of hyperfine fields and, where appropriate, with an additional quadrupole-splitting distribution. When one of the constituents of the hematite-maghemite mixtures was present in minor quantities, it could not be detected by the Mössbauer effect technique.

The Mössbauer spectra at variable temperature of two single-phase γ-Fe_2O_3 samples with extremely small particle sizes show the effect of superparamagnetism over a very broad temperature range. None of the average A- and B-site hyperfine parameters determined from fitting a single hyperfine-field distribution to the spectra, exhibit any unexpected temperature behaviour. Only at the lowest temperatures ($T \leq 55$ K), two distributed components were resolved from the spectra. Their relative areas, however, are not in good agreement with the expectations on the basis of the presumed cation distribution. In the external-field spectra the $\Delta m_I = 0$ transitions have not vanished, even for field strengths of up to 86 kOe. This effect is an intrinsic property of the maghe-

mite particles, indicating a strong spin canting with respect to the applied-field direction. The spectra could not be analyzed with two single sextet components nor with a hyperfine-field or canting-angle distribution. The external-field spectra were successfully reproduced using a bidimensional-distribution approach and acceptable values for the Mössbauer parameters were derived from the distribution profiles. The observed distributions are discussed and ascribed to the defect structure of the maghemites (unordered vacancy distribution on B-sites, large surface-to-bulk ratio, presence of OH^- groups). An important new finding is the correlation between the magnitude of the hyperfine field and the average canting angle for A-site ferric ions, whereas the B-site spins show a more uniform canting.

The Mössbauer parameters of the two hematite samples with MCD_{104} values of respectively 61.0 and 26.5 nm display a temperature variation which is very similar to that of small-particle hematites obtained from thermal decomposition of goethite. However, for a given MCD the Morin transition temperature for the latter samples is about 30 K lower. This has tentatively been ascribed to the different mechanisms of formation, presumably resulting in slightly larger lattice parameters for the hematite particles formed from goethite, thus shifting the Morin transition to lower temperatures.

Acknowledgements. The authors wish to thank Ir.W. Bohijn for the TEM photographs and Prof. R. Vochten for the DSC and TGA measurements. This work was supported by the Fund for Joint Basic Research (grant #2.0055.87) and in part by a NATO Collaborative Reserach Grant (#0370/86). One of the authors (EDG) gratefully acknowledges the financial support of the National Fund for Scientific Research, Belgium, and the Department of Physics of the Monash University which allowed him to perform experiments in the Mössbauer laboratory of that university.

References

Amin N, Arajs S (1987) Morin temperature of annealed submicronic α-Fe_2O_3 particles. Phys Rev B 35:4810–4811

Annersten H, Hafner SS (1973) Vacancy distribution in synthetic spinels of the series Fe_3O_4 – γ-Fe_2O_3. Z Kristallogr 137:321–340

Batis-Landoulsi H, Vergnon P (1983) Magnetic moment of γ-Fe_2O_3 microcrystals: morphological and size effect. J Mater Sci 18:3399–3403

Berkowitz AE, Schuele WJ, Flanders PJ (1968) Influence of crystallite size on the magnetic properties of acicular γ-Fe_2O_3 particles. J Appl Phys 39:1261–1263

Bernal JD, Dasgupta DR, Mackay AL (1957) Oriented transformations in iron oxides and hydroxides. Nature 180:645–647

Brett ME, Graham MJ (1986) An electron back-scattering Mössbauer spectroscopy study of thin magnetite films. J Magn Magn Mater 60:175–181

Bruzzone CL, Ingalls R (1983) Mössbauer-effect study of the Morin transition and atomic positions in hematite under pressure. Phys Rev B 28:2430–2440

Coey JMD (1971) Noncollinear spin arrangement in ultrafine ferrimagnetic crystallites. Phys Rev Lett 27:1140–1142

Coey JMD (1987) Noncollinear spin structures. Can J Phys 65:1210–1232

Coey JMD, Khalafalla D (1972) Superparamagnetic γ-Fe_2O_3. Phys Status Solidi (a) 11:229–241

de Bakker PMA, De Grave E, Persoons RM, Bowen LH, Vandenberghe RE (1990a) An improved, two-parameter distribution method for the description of the Mössbauer spectra of magnetic small particles in an applied field. J Phys: Meas Sci Technol 1:954–964

de Bakker PMA, De Grave E, Vandenberghe RE, Bowen LH (1990b) Mössbauer study of small-particle maghemite. Hyperfine Interactions 54:493–498

De Grave E, Vandenberghe RE (1990) Mössbauer study of the spin structure in natural hematites. Phys Chem Minerals 17:344–352

De Grave E, Chambaere D, Bowen LH (1983) Nature of the Morin transition in Al-substituted hematite. J Magn Magn Mater 30:349–354

De Grave E, Persoons RM, Chambaere DG, Vandenberghe RE, Bowen LH (1986) An ^{57}Fe Mössbauer effect study of poorly crystalline γ-FeOOH. Phys Chem Minerals 13:61–67

De Grave E, Bowen LH, Vochten R, Vandenberghe RE (1988) The effect of crystallinity and Al substitution on the magnetic structure and Morin transition in hematite. J Magn Magn Mater 72:141–151

Farell DM (1972) A study of the infrared absorption in the oxidation of magnetite to maghemite and hematite. Mines Branch Inv. Rept. 72-18: Dept. Energy Mines Res., Ottawa, Ontario, Canada, pp 44

Feitknecht W, Mannweiler U (1967) Der Mechanismus der Umwandlung von γ- zu α-Eisensesquioxid. Helv Chim Acta 50:570–581

Feitknecht W, Michaelis W (1962) Über die Hydrolyse von Eisen(III)-perchlorat-Lösungen. Helv Chim Acta 45:212–224

Goss CJ (1988) Saturation magnetization, coercitivity and lattice parameter changes in the system Fe_3O_4 – γ-Fe_2O_3 and their relationship to structure. Phys Chem Minerals 16:164–171

Greaves C (1983) A powder neutron diffraction investigation of vacancy ordering and covalency in γ-Fe_2O_3. J Solid State Chem 49:325–333

Haneda K, Morrish AH (1977a) Vacancy ordering in γ-Fe_2O_3 small particles. Solid State Commun 22:779–782

Haneda K, Morrish AH (1977b) On the hyperfine field of γ-Fe_2O_3 small particles. Phys Lett 64A:259–262

Jing J, Zhao F, Yang X, Gonser U (1990) Magnetic relaxation in nanocrystalline iron-oxides. Hyperfine Interactions 54:571–576

Klug HP, Alexander LE (1974) X-ray diffraction procedures for polycristalline and amorphous materials. Wiley, New York, pp 687–690

Koch CJW, Madsen BM, Mørup S (1986) Decoupling of magnetically interacting crystallites of goethite. Hyperfine Interactions 28:549–552

Kubo R (1952) The spin-wave theory of antiferromagnetics. Phys Rev 87:568–580

Lewis GK Jr, Drickamer HG (1966) Effect of high pressure on the lattice parameters of Cr_2O_3 and α-Fe_2O_3. J Chem Phys 45:224–226

Morrish AH, Clark PE (1974) Non-collinearity as a size effect in micropowders of γ-Fe_2O_3. Proc Int Conf Magn, Vol II, Moscow-USSR, Publishing House "Nauka", pp 180–184

Morrish AH, Haneda K, Schurer PJ (1976) Surface magnetic stucture of small γ-Fe_2O_3 particles. J Phys Colloq C6 37:301–305

Mørup S (1983) Magnetic hyperfine splitting in Mössbauer spectra of microcrystals. J Magn Magn Mater 37:39–50

Mørup S, Topsøe H (1976) Mössbauer studies of thermal excitations in magnetically ordered microcrystals. Appl Phys 11:63–66

Muench GJ, Arajs S, Matijevic E (1985) The Morin transition in small α-Fe_2O_3 particles. Phys Status Solidi (a) 92:187–192

Nininger RC Jr, Schroeer D (1978) Mössbauer studies of the Morin transition in bulk and microcrystalline α-Fe_2O_3. J Phys Chem Solids 39:137–144

Ochi A, Watanabe K, Kiyama M, Shinjo T, Bando Y, Takada T (1981) Surface magnetic properties of γ-Fe_2O_3 by ^{57}Fe Mössbauer emission spectroscopy. J Phys Soc Jpn 50:2777–2778

Okada T, Sekizawa H, Ambe F, Ambe S, Yamadaya T (1983) Magnetic and Mössbauer studies of Co adsorbed γ-Fe_2O_3. J Magn Magn Mater 31:903–904

Picone PJ, Haneda K, Morrish AH (1982) Dynamic and magnetic excitations in ultrafine particles. J Phys C: Solid State Phys 15:317–327

Pollard RJ (1990) The spin-canting anomaly in ferrimagnetic particles. J Phys: Condens Matter 2:983–991

Pollard RJ, Morrish AH (1987) High-field magnetism in non-polar γ-Fe_2O_3 recording particles. IEEE Trans Magn MAG-23:42–44

Ramdani A, Steinmetz J, Gleitzer C, Coey JMD, Friedt JM (1987) Perturbation de l'échange électronique rapide par les lacunes cationique dans $Fe_{3-x}O_4$ ($x \leq 0.09$). J Phys Chem Solids:217–228

Rendon JL, Cornejo J, De Arambarri P, Serna CJ (1983) Pore structure of thermally treated goethite (α-FeOOH). J Colloid Interface Sci 92:508–516

Sidhu PS (1988) Transformation of trace element-substituted maghemite to hematite. Clays Clay Minerals 36:31–38

Subrt J, Hanousek F, Zapletal V, Lipka J, Hucl M (1981) Dehydration of synthetic lepidocrocite (γ-FeOOH). J Thermal Anal 20:61–69

Takada T, Kiyama M, Shimizu S (1964) Morphological and crystallographical studies on the oriented transformation in γ-FeOOH and its decomposed oxides. Bull Inst Chem Res, Kyoto Univ 42:505–510

Tamura I, Hayashi M (1988) Magnetic interactions among closely packed γ-Fe_2O_3 microcrystals studied by Mössbauer spectroscopy. J Magn Magn Mater 72:285–294

Vandenberghe RE, De Grave E (1989) In: Long GJ, Grandjean F (eds) Mössbauer Spectroscopy Applied to Inorganic Chemistry, Vol 3. Plenum Press, New York, pp 59–182

Vaughan RW, Drickamer HG (1967) High-pressure Mössbauer studies on α-Fe_2O_3, $FeTiO_3$ and FeO. J Chem Phys 47:1530–1536

Verbeeck AE, De Grave E, Vandenberghe RE (1986) The effect of the particle morphology on the Mössbauer effect in α-Fe_2O_3. Hyperfine Interactions 28:639–642

Watari F, Van Landuyt J, Delavignette P, Amelinckx S (1979) Electron microscopic study of dehydration transformations. I. Twin formation and mosaic structure in hematite derived from goethite. J Solid State Chem 29:137–150

Watari F, Van Landuyt J, Delavignette P, Amelinckx S, Igita N (1982) X-ray peak broadening as a result of twin formation in some oxides derived by dehydration. Phys Status Solidi (a) 73:215–224

Wivel C, Mørup S (1981) Improved computational procedure for evaluation of overlapping hyperfine parameter distributions in Mössbauer spectra. J Phys E: Sci Instrum 14:605–610

Wolska E, Baszynski J (1986) Prereactional transformations in the topotatic conversion γ-FeOOH$\rightarrow\gamma$-Fe_2O_3. Phys Status Solidi (a) 95:87–92